Implementation of Majorization-Minimization (MM) Algorithm for 3D Total Variation Minimization in DBT Image Reconstruction

Adem Polat, Nuno Matela, Ana Margarida Mota, and Isa Yildirim

***Abstract*—Digital Breast Tomosynthesis (DBT) is a developing imaging modality which produces 3D images of a breast. Iterative image reconstruction techniques, such as Algebraic reconstruction technique (ART), have been proposed to help increasing success in detecting masses and micro-calcifications. To enhance the quality of reconstructed image, total variation (TV) minimization was applied to the images reconstructed by ART. Nowadays, the number of published papers dealing with 3D TV minimization on ART (ART+TV$_{3D}$) tends to increase. On the other hand, in the signal processing literature, a new majorization-minimization (MM) algorithm on TV denoising is described for an N-point *x(n)* as 1D signal. According to our literature review, this 1D MM algorithm has not been applied to DBT studies yet. In this paper, we propose a method to combine MM$_{1D}$ algorithm with ART+TV$_{3D}$: "ART+TV$_{3D}$+MM$_{1D}$". Both quantitative and qualitative analyses of the proposed method ART+TV$_{3D}$+MM$_{1D}$, ART+TV$_{3D}$, and ART are performed for a phantom that mimics 3D breast and a real 3D breast phantom with 301x236x8-dimensions.**

***Keywords*—digital breast tomosynthesis, iterative reconstruction, total variation, majorization-minimization**

I. Introduction

THERE are two types of methods, including analytical and iterative algorithms to reconstruct tomosynthesis images for detecting masses and micro-calcifications. Algebraic reconstruction technique (ART), an iterative image reconstruction method, is used to reconstruct 3D image of a breast. It is becoming one viable alternative method to the conventional image reconstruction techniques, such as filtered back projection (FBP) [1], [2]. ART reconstructs a few projections acquired from a limited view angle scanning of a breast. In the last decade, DBT studies have largely addressed the problem of obtaining reconstructed image from a few projections, which means a highly under sampled data. This can be done via compressed sensing (CS) [3], [4]. Total variation (TV) [5], one of the operators of CS, minimizes l_1 or l_2 norm of the gradient of the image, and this idea was applied to the tomosynthesis imaging problem. TV minimization can be applied to the tomosynthesis images reconstructed by ART to address limitations of the problem such as out of focus slice blurring. Nowadays, while the majority of the studies deal with 2D TV minimization, only few of them mention 3D TV minimization [6]. On the other hand, in the signal processing literature, a new majorization-minimization (MM) algorithm [7] on TV denoising is described for an N-point *x(n)* as 1D signal [8]. The (MM) algorithm is an optimization method which exploits the convexity of a function in order to find its maxima or minima to optimize a developed iterative algorithm [7],[9].

To the best of our knowledge, this MM$_{1D}$ algorithm has not been applied to DBT studies yet. In this paper, we propose and implement an application of MM$_{1D}$ algorithm to 3D DBT imaging problem. Both quantitative and qualitative analyses of the proposed method called "TVMM", ART+TV$_{3D}$ called "TV3D", and ART are carried out for a phantom that mimics 3D breast and for real digital breast images, as well.

II. Methods

The proposed method called "TVMM" was implemented for a phantom with dimensions 61x61x9 that simulates 3D breast roughly and for DBT images of CD Pasmam 1054 phantom [10] scanned via Siemens MAMMOMAT [11], as well. In TVMM method, MM$_{1D}$ algorithm is applied to ART+TV$_{3D}$ volumes in each iteration.

A. Applications of Analytical Phantom

Nine slices of analytical phantom with dimensions 61x61 that simulates a 3D breast is illustrated in Fig.1. Layer-3 is chosen as the layer of interest (LOI) due to the existence of fine details in this layer.

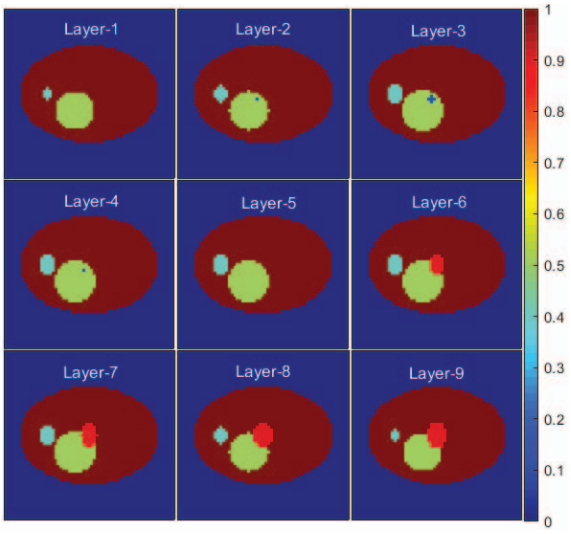

Fig.1. 9 layers of the mimic of a 3D breast (61x61x9).

Manuscript received December 5, 2016. This work has been supported in part by Fundação para a Ciência e a Tecnologia - Portugal (Project Pest-OE/SAU/IU0645/2013) and TUBITAK, the Scientific and Research Council of Turkey, under the grant 111E086.

A. Polat is with Istanbul Technical University, Faculty of Electrical and Electronics Engineering, Institute of Informatics, 34469 Istanbul, Turkey and he is currently with Harvard-MIT, Division of Health Sciences and Technology, Massachusetts Institute of Technology, Cambridge, MA, 02139, USA (e-mail: apolat@mit.edu and polatadem@itu.edu.tr

N. Matela is with Universidade de Lisboa, Faculdade de Ciencias, Instituto de Biofisica e Engenharia Biomedica, 1749-016 Lisbon, Portugal (e-mail: nmatela@gmail.com).

A.M.Mota is with Universidade de Lisboa, Faculdade de Ciencias, Instituto de Biofisica e Engenharia Biomedica, 1749-016 Lisbon, Portugal (e-mail: ninimota87@gmail.com

I. Yildirim is with Istanbul Technical University, Faculty of Electrical and Electronics Engineering, Institute of Informatics, 34469 Istanbul, Turkey and he is also with Electrical and Electronics Eng. Dept. of Abdullah Gul University, Turkey and College of Engineering of University of Illinois, Chicago, USA (e-mail: iyildirim@itu.edu.tr).

978-1-5090-1642-6/16/$31.00 ©2016 IEEE

We have simulated the acquisition of 25 projections via Siddon's algorithm [12] and calculated the system matrix by the same method. The phantom was scanned at angles of (-25.19º, -22.98º, -20.78º, -19.12º, -17.22º, -15.14º, -13.45º, -11.41º, -9.54º, -7.48º, -5.63º, -3.55º, -1.92º, 0.29º, 2.23º, 4.00º, 5.79º, 7.84º, 9.99º, 11.64º, 13.49º, 15.6º, 17.76º, 18.92º, 21.77º) in the same way as the real geometry of DBT system of Siemens MAMMOMAT.

ART formulated in (1) [13] was used to reconstruct these 25 projections by applying 10 iterations. The voxels of the phantom are updated ray by ray for each projection, and updating is repeated for all 25 projections to complete a single iteration. During each iteration of ART+TV_{3D} method, 3D TV minimization, expressed in (2) [6], is applied to 3D data reconstructed by ART.

$$X_j^{(k+1)} = X_j^{(k)} + \left[\left(Y_i - \sum_{m=1}^{M} a_{im} X_m^{(k)}\right) \Big/ \sum_{m=1}^{M} a_{im}^2\right] \cdot a_{ij}, \quad \text{for } \begin{matrix} i=1,2,3,\ldots,N \\ j=1,2,3,\ldots,M \end{matrix} \tag{1}$$

$$TV_{3D}(\mathbf{X}) = \sum_{k}^{K}\sum_{j}^{J}\sum_{i}^{I}\sqrt{\left(X_{i,j,k} - X_{i-1,j,k}\right)^2 + \left(X_{i,j,k} - X_{i,j-1,k}\right)^2 + \left(X_{i,j,k} - X_{i,j,k-1}\right)^2} \tag{2}$$

In the proposed TVMM (ART+TV_{3D}+MM_{1D}) method, we apply MM_{1D} algorithm after 3D TV minimization step at each iteration. The major difference here is that 3D data is reshaped to 1D as input of TVMM algorithm after 3D TV minimization. The second point is that TVMM algorithm has another inner iteration process in itself. We adapted the open source matlab program of MM_{1D} algorithm developed by [8] to our problem with 5 iterations. All simulations were implemented on Matlab R2015b.

B. Applications of Real DBT Images

CD Pasmam 1054 phantom manufactured by Southern Scientific Ltd, West Sussex United Kingdom was scanned with a Siemens MAMMOMAT Inspiration system (Siemens AG, Healthcare Sector Erlangen, Germany) installed in a clinical facility (Hospital da Luz S.A., Lisbon, Portugal). The equipment acquires 25 projections with short x-ray pulses with 28 kVp and 056 mAs.

The reference projection taken at 056 mAs dose at angle of 0.29º (center of moving arm) and FBP image of Siemens MAMMOMAT are shown in Fig. 2.

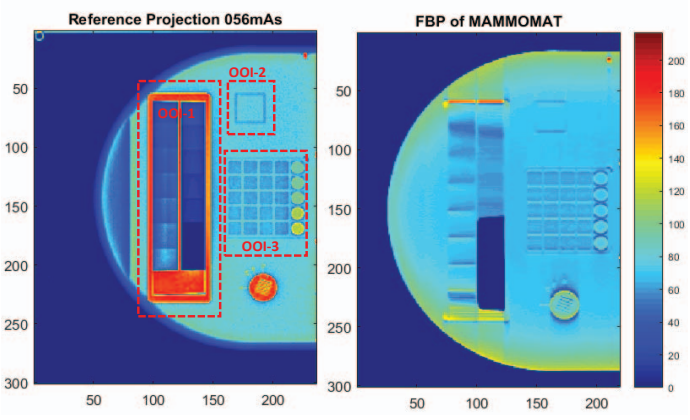

Fig.2. The reference projection at angle of 0.29º (left) and FBP (right).

We run all algorithms for down sampled projections as 301x236 pixels. We reconstruct 25 down sampled projections as 8 slices in this project and compare our results of reconstructed images with down sampled of 300x220 pixels and 8 slices images of Siemens MAMMOMAT's FBP.

III. Results and Conclusion

A. The Results of Analytical Phantom

The results of LOI (3th Layer) of ART, TV3D, and TVMM can be visually compared in Fig.3. The visual interpretation can be done by focusing on two objects of interest (OOI-A and OOI-B). While obtaining similar results in both TV3D and TVMM, both methods outperformed ART. Among all methods, TVMM has the lowest background noise level.

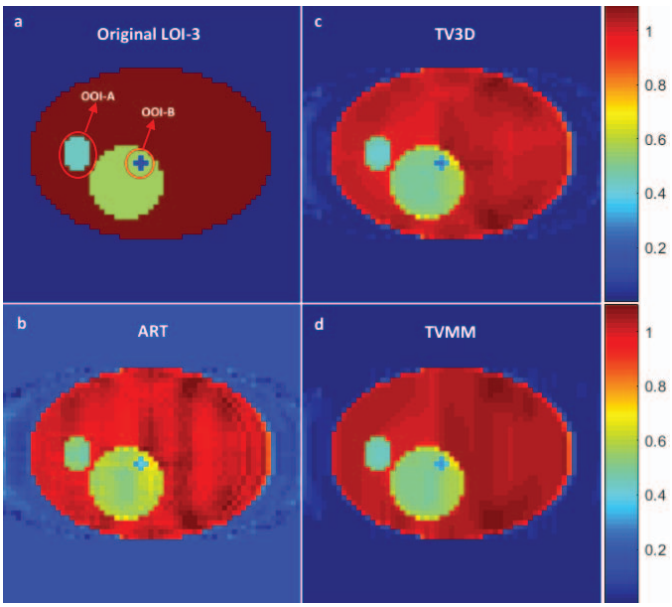

Fig.3. Original LOI (a), the reconstructed LOI via ART (b), TV3D implementation of ART (c), and TVMM implementation of TV3D (d).

To evaluate the performance of TVMM method by comparing to TV3D and ART, apart from qualitative assessment; quantitative metrics such as signal to noise ratio (SNR) and structural similarity (SSIM) of the LOI are examined as well. The behaviors of SNR and SSIM versus the number of iteration are given in Fig. 4 and Fig. 5, respectively.

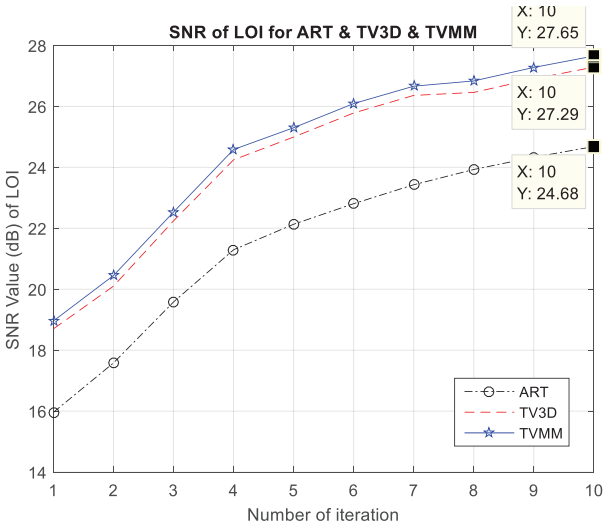

Fig.4. SNR (dB) values of ART, TV3D, and TVMM.

Structure SIMilarity (SSIM), introduced by [14] as a new metric, offers a metric which has a closer match with the human vision. Matlab code for SSIM can be accessed on [15].

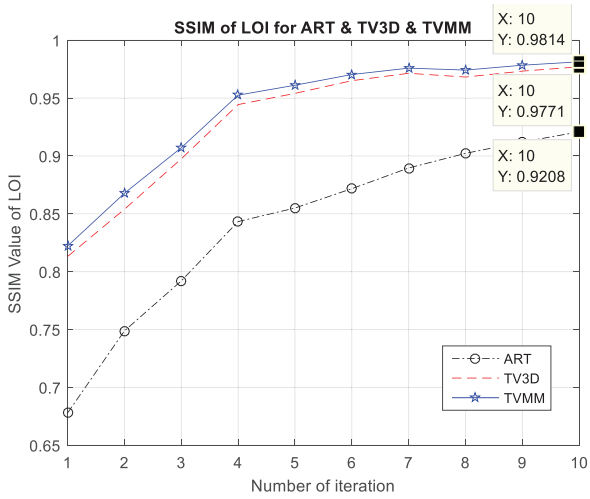

Fig.5. SSIM values of ART, TV3D, and TVMM.

At the end of the 10th iteration, while SSIM value of TV3D is 0.9771, TVMM reaches to 0.9814 SSIM value. Furthermore, SNR (dB) values of TV3D and TVMM are 27.29 and 27.65, respectively. ART performed the poorest for both metrics. In conclusion, the proposed method TVMM helps in obtaining superior results in terms of SNR and SSIM values compared to TV3D.

B. The Results of Real DBT Images

Reconstructed images of 25 projections of real breast phantom CD Pasmam 1054 by FBP-Siemens MAMMOMAT, ART, TV3D, and TVMM for 056 mAs are shown in Fig. 6.

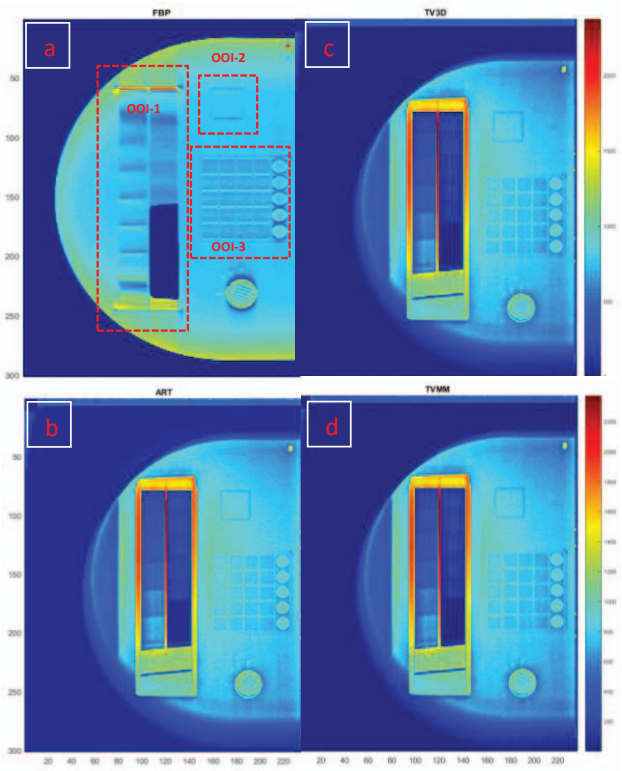

Fig. 6. FBP (a), ART (b), TV3D (c), and TVMM (d) for 56 mAs.

OOI-1 (Object of Interest-1) drawn on the reference projection in Fig.2 is blurred in the reconstructed image by the FBP compared to the reconstructed images by ART, TV3D, and TVMM (see Fig. 6). When we zoom in OOI-2 in Fig. 7, TV3D and TVMM provide better images in terms of preserving the edges than the FBP and ART methods.

Our proposal method TVMM makes the sharpness of OOI-2 increase. Additionally, it is spied on that the quality of detectability of the square-shape is much better for our applications than FBP. In the method, TVMM that we propose has similar quality as TV3D. Moreover, it is quite obvious that TVMM is much better quality than ART.

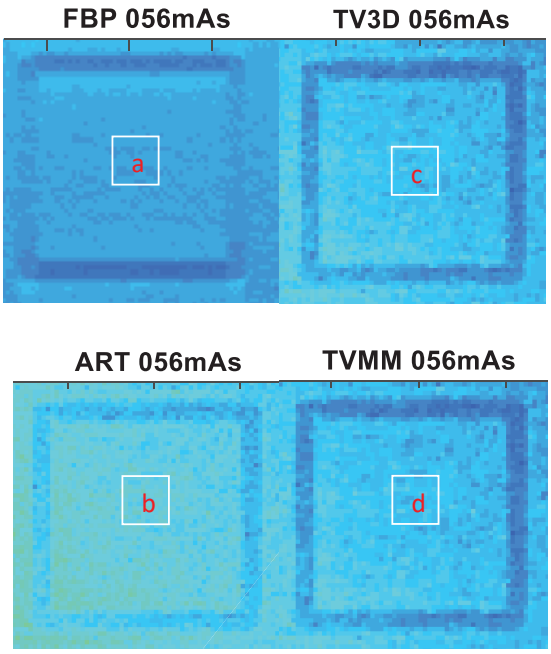

Fig.7. Zoom in IOO-2; FBP (a), ART (b), TV3D (c), and TVMM (d).

For the quantitative analysis of the methods, CNR (contrast to noise ratio) defined in (3) and 1-D profile explained on next page of the reconstructed images were used.

$$CNR = \left(\mu_{ROI} - \mu_{Background}\right) / \sigma_{Background} \qquad (3)$$

where μ_{ROI} and $\mu_{Background}$ are mean values of ROI and background selected on an OOI respectively, and $\sigma_{Background}$ stands for standard deviation value of background.

ROI-1 (in OOI-1), ROI-2 (in OOI-2) and their background areas are illustrated in Fig. 8. The CNRs of ROI-1 and ROI-2 of the methods are compared in the Table. I.

TABLE I. CNR VALUES OF FBP, ART, TV3D, AND TVMM

	FBP	ART	TV3D	TVMM
CNR of ROI-1	1,034	39,514	42,292	42,208
CNR of ROI-2	1,528	1,146	1,124	1,126

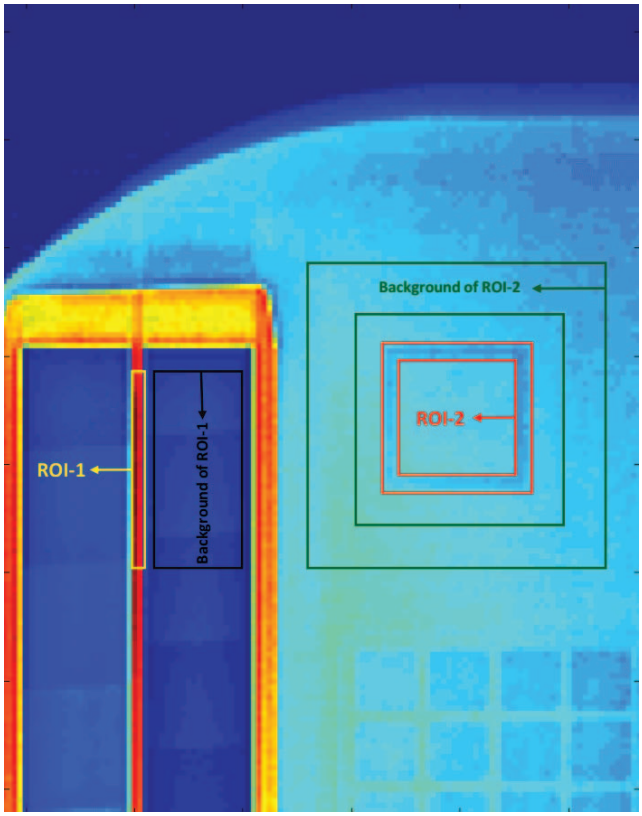

Fig.8. ROI-1 (yellow), background of ROI-1 (black), ROI-2 (red), and background of ROI-2 (green).

CNR values of ROI-2 of TV3D and TVMM are less than the one of the FBP. This can be explained by the effect of down sampling, carried in the images reconstructed by the FBP, in smoothing the background. On the other hand, CNR values of ROI-1 of TV3D and TVMM are way better than the one of the FBP method.

For the 1-D profile comparison, the horizontal profile shown by a red line in Fig. 9 was chosen. 1-D profiles of the FBP, ART, TV3D, and TVMM are given in Fig. 10. TVMM and TV3D show better performance than ART by generating smoother images in the uniform areas and than FBP by creating sharper edges between the uniform areas.

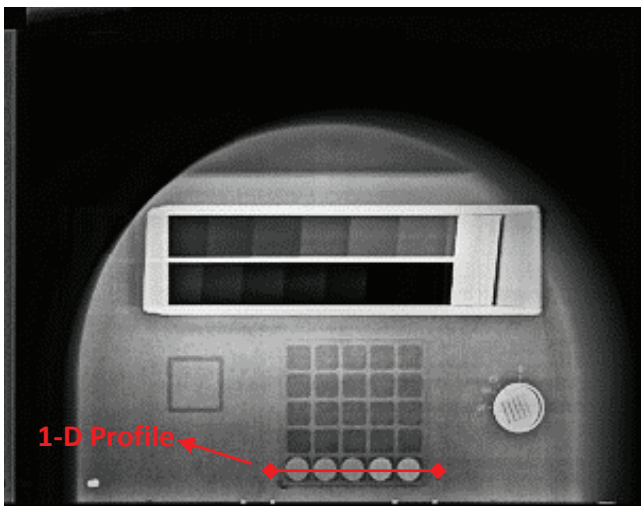

Fig.9. 1-D profile in IOO-3.

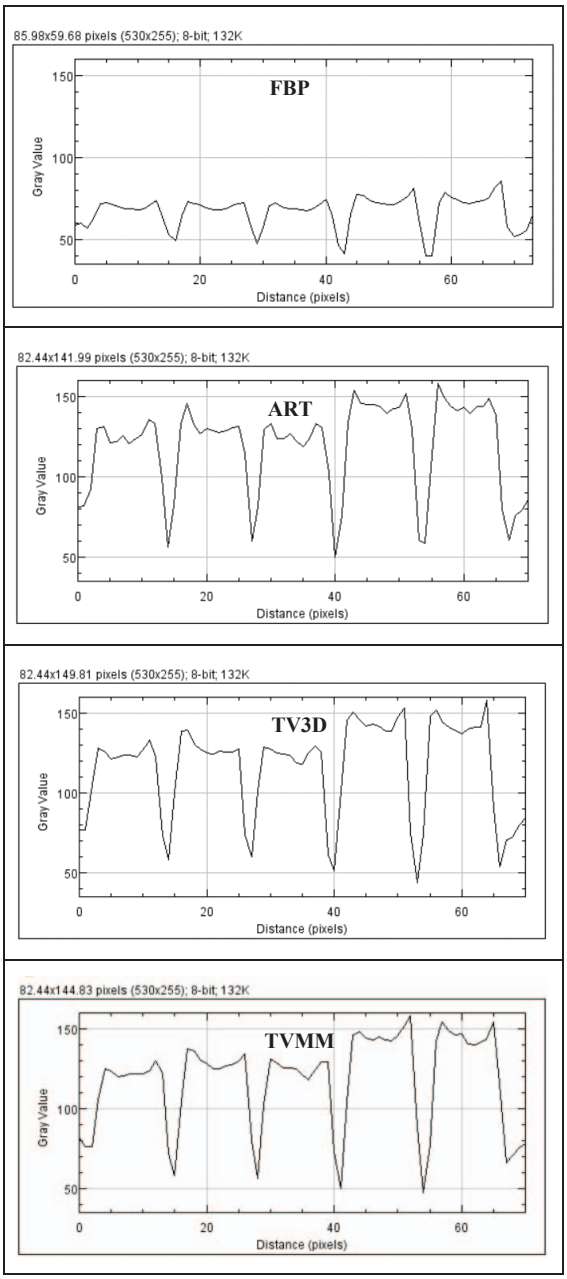

Fig.10. 1-D profiles of the FBP (1th row)), ART (2nd row), TV3D (3th row), and TVMM (4th row).

In this work, a new majorization-minimization (MM) algorithm on TV denoising has been adapted to DBT image reconstruction problem by applying it to images reconstructed by ART+TV_{3D}. The proposed method was compared by the FBP of Siemens MAMMOMAT, ART, and ART+TV_{3D} both qualitatively and quantitatively. Based on the visual inspection, SNR value, CNR value, SSIM value, and 1-D profile, the proposed and TV3D methods provided superior results over the FBP method of Siemens MAMMOMAT, and ART method.

REFERENCES

[1] M. Ekstrom, Digital Image Processing Techniques. Orlando-Florida: Academic Press, 1984, pp. 142-166.
[2] M. Helvie, "Digital mammography imaging: breast tomosynthesis and advanced applications", Radiol Clin North Am, vol. 48, no. 5, pp. 917–929, 2010.
[3] Y. Park, H. Cho, U. Je, H. Cho, C. Park, H. Lim, K. Kim, G. Kim, S. Park, T. Woo and S. Choi, "Evaluation of the image quality in digital breast tomosynthesis (DBT) employed with a compressed-sensing (CS)-based reconstruction algorithm by using the mammographic accreditation

phantom", Nuclear Instruments and Methods in Physics Research A 804, vol. 804, pp. 72-78, 2015.
[4] E. Candes and M. Wakin, "An Introduction To Compressive Sampling", IEEE Signal Processing Magazine,1053-5888/08/$25.0, pp. 21-30, 2008.
[5] L.Rudin, S. Osher and E. Fatemi, "Nonlinear total variation based noise removal algorithms", Physica D, vol. 60, pp. 259-268, 1992.
[6] M. Ertas, I. Yildirim, M. Kamasak and A. Akan, "Digital breast tomosynthesis image reconstruction using 2D and 3D total variation minimization", BioMedical Engineering OnLine,vol.12,no.1,p.112, 2013.
[7] M. Figueiredo, J. Bioucas-Dias and R. Nowak, "Majorization - Minimization Algorithms for Wavelet-Based Image Restoration", IEEE Transactions on Image Processing, vol. 16, no. 12, pp. 2980-2991, 2007.
[8] I. Selesnick, "Total Variation Denoising (MM Algorithm)", Eeweb.poly.edu, 2014. [Online]. Available: http://eeweb.poly.edu /iselesni/lecture_notes/TVDmm. [Accessed: 01- Apr- 2016].
[9] D. Hunter and K. Lange, "A Tutorial on MM Algorithms", The American Statistician, vol. 58, no. 1, pp. 30-37, 2004.
[10] Southern Scientific Ltd, "CD PASMAM 1054 Datasheet ".
[11] Siemens AG, "MAMMOMAT Inspiration - Tomosynthesis Option ", Vol.January 2016 (available on: http://www.accessdata.fda.gov/ cdrh_docs/pdf14/P140011c.pdf, Last accessed January 2016).
[12] R. Siddon, "Fast calculation of the exact radiological path for a three-dimensional CT array", Med. Phys., vol. 12, no. 2, p. 252, 1985.
[13] M. Ertas, I. Yildirim, M. Kamasak and A. Akan, "An iterative tomosynthesis reconstruction using total variation combined with non-local means filtering", BioMedical Engineering OnLine, vol. 13, no. 1, p. 65, 2014.
[14] Z. Wang, A. Bovik, H. Sheikh and E. Simoncelli, "Image Quality Assessment: From Error Visibility to Structural Similarity", IEEE Transactions on Image Processing, vol. 13, no. 4, pp. 600-612, 2004.
[15] Z. Wang, 2016. [Online]. Available: https://ece.uwaterloo.ca/~ z70wang/research/ssim/. [Accessed: 12- Apr- 2016].